Commun Nonlinear Sci Numer Simulat 16 (2011) 3887–3895

Contents lists available at ScienceDirect

Commun Nonlinear Sci Numer Simulat

journal homepage: www.elsevier.com/locate/cnsns

Short communication

Evolutionary dynamics of a system with periodic coefficients

Richard H. Rand [a,b,*], Max Yazhbin [c], David G. Rand [d]

[a] Dept. of Mathematics, Cornell University, Ithaca, NY 14853, United States
[b] Dept. of Mechanical and Aerospace Engineering, Cornell University, Ithaca, NY 14853, United States
[c] Dept. of Chemical and Biomolecular Engineering, Cornell University, Ithaca, NY 14853, United States
[d] Program for Evolutionary Dynamics, Harvard University, Cambridge, MA 02138, United States

ARTICLE INFO

Article history:
Received 11 January 2011
Accepted 18 February 2011
Available online 27 February 2011

Keywords:
Replicator equation
Parametric excitation
Evolutionary dynamics

ABSTRACT

We investigate a problem in evolutionary game theory based on replicator equations with periodic coefficients. This approach to evolution combines classical game theory with differential equations. The RPS (Rock-Paper-Scissors) system studied has application to the population biology of lizards and to bacterial dynamics. The presence of periodic coefficients models variations in the environment due to seasonal effects and results in parametric excitation which is studied through the use of perturbation series and numerical integration.

1. Introduction

Evolution is the fundamental unifying principle of biology. In its essence, natural selection dictates that traits which cause an organism to produce more offspring become more common in the population. The field of evolutionary game theory uses mathematics to formalize the dynamics of evolution [3,7]. These evolutionary models provide a powerful set of tools for predicting what traits will be favored by natural selection in particular settings.

Evolutionary game theory is not limited to genetic evolution, in which organisms pass their genes onto offspring [6]. These models can also describe 'cultural evolution' or social learning, where people copy strategies of others with higher payoffs. Recent work has demonstrated the ability of evolutionary models to quantitatively reproduce human behavior in economic experiments, out-performing the predictions of classical economic models [2,8].

In game theoretic models, a set of players each chooses a 'strategy'. Each player then earns a payoff based on her strategy as well as the strategy chosen by one or more others. For example, consider the game 'Rock–Paper–Scissors' (RPS). Players interact in pairs, and each player chooses one of three strategies: rock (R), paper (P) or scissors (S). Rock beats scissors; thus if you pick R while your opponent picks S, you earn a positive payoff (say + 1). If you choose S while your opponent chooses R, however, you 'lose' and receive a negative payoff (say − 1). The full set of payoffs is often described using a payoff matrix, where the payoff of the row player is indicated. The payoff matrix for the simplest RPS game is thus given by

$$\begin{array}{c} \\ R \\ P \\ S \end{array} \begin{array}{c} \begin{array}{ccc} R & P & S \end{array} \\ \begin{bmatrix} 0 & -1 & +1 \\ +1 & 0 & -1 \\ -1 & +1 & 0 \end{bmatrix} \end{array} \tag{1}$$

* Corresponding author at: Dept. of Mathematics, Cornell University, Ithaca, NY 14853, United States.
E-mail address: rhr2@cornell.edu (R.H. Rand).

1007-5704/$ - see front matter © 2011 Elsevier B.V. All rights reserved.
doi:10.1016/j.cnsns.2011.02.023

In the context of evolutionary game theory, these payoffs represent reproductive success (i.e. number of offspring). Strategies which earn higher payoffs thus become more common over time.

One particularly popular approach to formalizing this evolutionary dynamic is the 'replicator equation' [10]. The replicator equation uses differential equations to describe changes in the abundance of a finite set of N strategies in an infinitely large population of players. We define x_i as the abundance of strategy i, i.e. the fraction of players in the population using strategy i. (Note that *abundance* is often called *frequency* in the literature of evolutionary dynamics. In this paper we reserve the latter term for frequency of oscillation.) Therefore

$$\sum_{i=1}^{N} x_i = 1 \tag{2}$$

In its standard form, the replicator equation assumes that every player is equally likely to interact with every other player. Thus for a game where players interact in pairs, the expected payoff of an individual playing strategy i is given by

$$f_i = \sum_{j=1}^{N} A_{ij} x_j \tag{3}$$

where A_{ij} is the payoff of strategy i playing against strategy j. Note that the expected payoff of a given strategy depends on the abundances of each strategy in the population. A strategy which earns a high payoff in one setting may score poorly in others. For example, in RPS, an R player would earn a high payoff in a population where S is common, but would earn a low payoff in a population where P is common.

The replicator equation stipulates that strategies with higher than average payoff increase in abundance, while strategies with lower than average payoff decrease in abundance. The rate of change of the abundance of strategy i is given by

$$\dot{x}_i = x_i(f_i - \Phi) \tag{4}$$

where Φ is the average payoff, given by

$$\Phi = \sum_{j=1}^{N} x_j f_j \tag{5}$$

Eq. (4) can then be used to study the evolutionary dynamics of a particular game. In this paper, we focus on the RPS game. Although Rock–Paper–Scissors may seem like a trivial child's game, it in fact serves as a model of many interesting systems in biology and social science. For example, mating behavior of the male side-blotched lizard *Uta stansburiana* displays a rock-paper-scissors dynamic [11]. There are three different genetic variates (genotypes) of males in this lizard species: those that have large territories; those that have small territories; and 'sneakers' which have no territory and instead pose as females and invade the territories of other males. Males with large territories cannot closely guard their females and so are outcompeted by sneaker males. Sneaker males have no females of their own and so are outcompeted by males with small territories, who can effectively guard their females. And males with small territories are out-competed by males with large territories because the latter control more females. Thus these three strategies display a RPS dynamic.

Another example comes from the bacteria *Escherichia coli* [4]. The normal 'wild-type' strain of bacteria forms a RPS dynamic with two other strains: a toxic strain which produces both a toxin and an antidote to the toxin, and a resistant strain which produces only the antidote. The toxin kills the wild-type bacteria, and so the toxic strain can invade the wild-type. But once the population consists entirely of toxic bacteria, there is no advantage to producing the toxin (which requires energy). Therefore the resistant strain can invade the toxic strain. Yet once the population consists only of resistant bacteria, there is no reason to produce the antidote (which also requires energy). Thus the wild-type strain can invade the resistant strain.

In this paper, we extend the standard RPS model to consider periodic variation in payoffs. Such effects could be due to annual changes in fitness due to seasonal weather changes. Periodic coefficients in replicator dynamics have been previously treated in [1]. There it is shown that for sufficiently fast oscillations, periodic coefficients in a two-player game can be reduced to constant coefficients in a multi-player game, and that this can create stable equilibria with non-zero abundances of multiple strategies (co-existence).

2. Model

We generalize the RPS payoff matrix (1) by allowing two of the coefficients to depend explicitly on time:

$$\begin{array}{c} \\ R \\ P \\ S \end{array} \begin{array}{c} \begin{array}{ccc} R & P & S \end{array} \\ \begin{bmatrix} 0 & -1-\epsilon\cos\omega t & +1+\epsilon\cos\omega t \\ +1 & 0 & -1 \\ -1 & +1 & 0 \end{bmatrix} \end{array} \tag{6}$$

where ϵ, the magnitude of the forcing function, is a small parameter, $\epsilon \ll 1$, and where ω is the frequency of the forcing function.

The expected payoffs (3) become:

$$f_1 = (1 + \epsilon \cos \omega t)(-x_2 + x_3) \tag{7}$$

$$f_2 = x_1 - x_3 \tag{8}$$

$$f_3 = -x_1 + x_2 \tag{9}$$

The average payoff Φ given by Eq. (5) becomes:

$$\Phi = \sum_{j=1}^{N} x_j f_j = x_1(x_3 - x_2)\epsilon \cos \omega t \tag{10}$$

and the replicator Eq. (4) become:

$$\dot{x_1} = x_1(f_1 - \Phi) = x_1(x_3 - x_2)[1 + (1 - x_1)\epsilon \cos \omega t] \tag{11}$$

$$\dot{x_2} = x_2(f_2 - \Phi) = x_2[(x_1 - x_3) + x_1(x_2 - x_3)\epsilon \cos \omega t] \tag{12}$$

$$\dot{x_3} = x_3(f_3 - \Phi) = x_3[(x_2 - x_1) + x_1(x_2 - x_3)\epsilon \cos \omega t] \tag{13}$$

Eqs. (11)–(13) exhibit the invariant manifold (2) which may be pictured as a simplex in the first octant in x_1–x_2–x_3 space, see Fig. 1. Note that the vertices of this simplex, (1,0,0), (0,1,0) and (0,0,1), are equilibria of Eqs. (11)–(13).

3. Properties of the model

Eqs. (11) and (12) may be simplified by eliminating x_3 through the use of Eq. (2), giving:

$$\dot{x_1} = x_1(1 - 2x_2 - x_1)[1 + (1 - x_1)\epsilon \cos \omega t] \tag{14}$$

$$\dot{x_2} = x_2(x_2 + 2x_1 - 1 + [x_1(2x_2 + x_1 - 1)]\epsilon \cos \omega t) \tag{15}$$

Eqs. (14) and (15) may be viewed as a flow on the x_1–x_2 plane, see Fig. 2. As in Fig. 1, the vertices of the simplex in Fig. 2, namely (1,0), (0,1) and (0,0), are equilibria for Eqs. (14) and (15). In addition, there is another equilibrium at (1/3,1/3). The lines which bound the simplex are invariant manifolds for the flow (14) and (15). These are $x_1 = 0$, $x_2 = 0$ and $x_1 + x_2 = 1$, the last being equivalent to $x_3 = 0$ in view of Eq. (2). Thus any motion which starts inside the simplex must remain inside for all time.

In the case that $\epsilon = 0$, the system (14) and (15) admits a first integral:

$$x_1 x_2(1 - x_1 - x_2) = \text{constant} \tag{16}$$

See Fig. 3 where the integral curves (16) are displayed for various values of the constant. Each of these curves represents a motion which is periodic in time. For $\epsilon > 0$, the presence of the time-varying periodic term $\epsilon \cos \omega t$ destroys the first integral

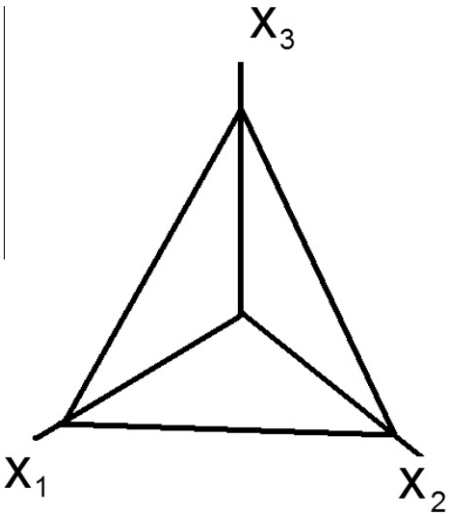

Fig. 1. Eqs. (11)–(13) exhibit the invariant manifold (2). That is, motions which start on the simplex (the triangular region) remain on it for all time.

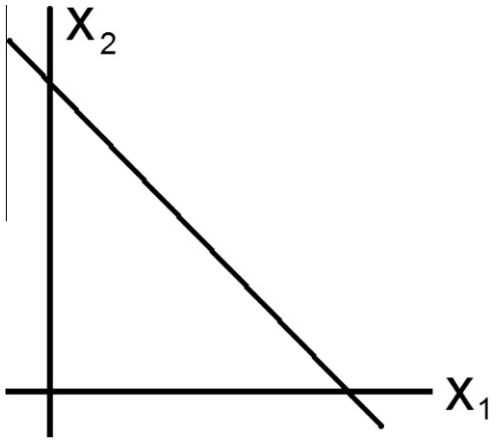

Fig. 2. Eqs. (14) and (15) may be viewed as a flow on the x_1–x_2 plane.

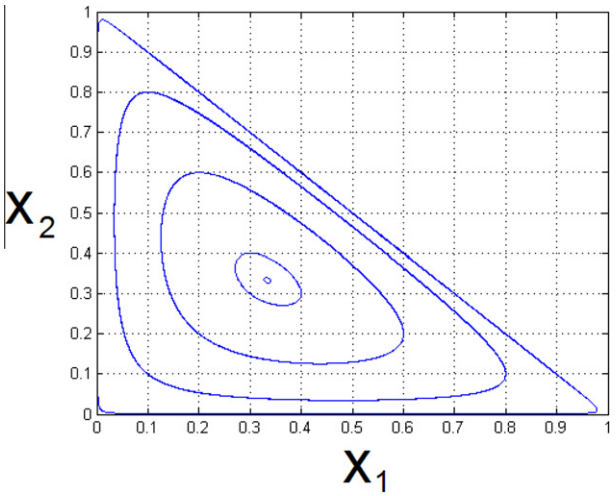

Fig. 3. Integral curves from Eq. (16) for $\epsilon = 0$. Each of these curves represents a motion which is periodic in time.

(16). Numerical integration shows that for small values of ϵ the periodic motions of Eq. (16) are typically replaced by quasiperiodic motions, see Fig. 4. In particular, motions starting near the equilibrium point $(1/3, 1/3)$ typically remain near it as in Fig. 4. An exception occurs for certain values of the system parameters ϵ and ω. See Fig. 5 which displays a numerically integrated motion starting near $(1/3, 1/3)$ for parameters $\epsilon = 0.1$, $\omega = 1.154$. Note that here a motion which starts near the equilibrium $(1/3, 1/3)$ travels far away from it. In what follows we seek to explain this phenomenon through a study of the stability of the equilibrium $(1/3, 1/3)$.

4. Stability of motion

To investigate the stability of the equilibrium at $(1/3, 1/3)$, we set

$$x_1 = x + \frac{1}{3}, \quad x_2 = y + \frac{1}{3} \tag{17}$$

we substitute these into Eqs. (14) and (15), and we linearize in x, y, giving:

$$\dot{x} = -\left(\frac{x + 2y}{3}\right) - \frac{2}{9}(2y + x)\epsilon \cos \omega t \tag{18}$$

$$\dot{y} = \left(\frac{2x + y}{3}\right) + \frac{1}{9}(2y + x)\epsilon \cos \omega t \tag{19}$$

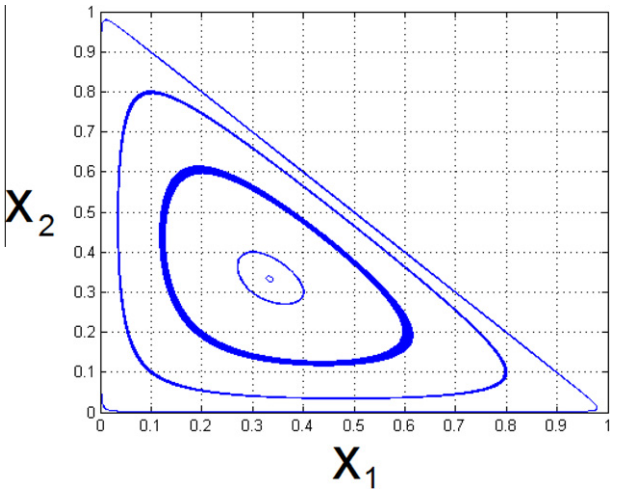

Fig. 4. Motions of Eqs. (14) and (15) for $\epsilon = 0.02$ and $\omega = 1$ obtained by numerical integration. Here the periodic motions of Fig. 1 are replaced by quasiperiodic motions. Note that motions starting near the equilibrium point (1/3, 1/3) remain near it.

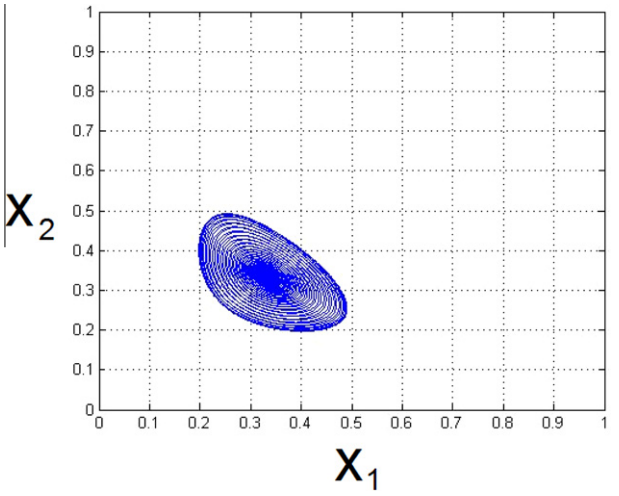

Fig. 5. Motion of Eqs. (14) and (15) for $\epsilon = 0.1$ and $\omega = 1.154$ for initial conditions $x_1 = x_2 = 0.3333$ obtained by numerical integration. Note that here a motion which starts near the equilibrium (1/3, 1/3) travels far away from it.

Next we define a new time variable $\tau = \omega t$ and we transform this first order system of ODEs into a single second order ODE by differentiating (18) and substituting expressions for $\dot{y}$ from (19) and for y from (18), giving:

$$f_1 x'' + f_2 x' + f_3 x = 0 \tag{20}$$

where primes represent differentiation with respect to τ, and where

$$f_1 = 3 + 2\epsilon \cos\tau \tag{21}$$

$$f_2 = 2\epsilon \sin\tau \tag{22}$$

$$f_3 = \left(\frac{3 + 2\epsilon\cos\tau}{3\omega}\right)^2 \tag{23}$$

Eq. (20) is an example of a linear differential equation with periodic coefficients and is a variant of Ince's equation [5,9]. It contains two parameters, ω and ϵ and results may therefore be viewed in the ω–ϵ parameter plane. For a given pair of parameters there are two possibilities: either all solutions are bounded, in which case the point (ω, ϵ) is said to be *stable*, or an unbounded solution exists and the point is called *unstable*. We are interested in *transition curves* which separate regions

of stability from regions of instability in the ω–ϵ plane. A straightforward line of reasoning leads us to expect tongues of instability to emanate from the points $\omega = \frac{2}{n\sqrt{3}}$, $n = 1,2,3,\ldots$ on the ω-axis, as follows.

A result from *Floquet theory* [12,9] states that equations of the form of Hill's equation,

$$\frac{d^2z}{d\tau^2} + F(\tau)z = 0, \quad F(\tau + T) = F(\tau) \tag{24}$$

have periodic solutions of period T or $2T$ on their transition curves, where T is the period of the coefficient $F(\tau)$. However, Eq. (20) is not of the form of Hill's Eq. (24). Nevertheless, if we set

$$x = \sqrt{3 + 2\epsilon\cos\tau}\quad z \quad (|\epsilon| < 3/2) \tag{25}$$

then it turns out that Eq. (20) becomes a Hill's Eq. (24) on $z(\tau)$, with the following coefficient $F(\tau)$:

$$F(\tau) = \frac{54 + (108 - 54\omega^2)\epsilon\cos\tau + [36 - 45\omega^2 + (36 + 9\omega^2)\cos\tau]\epsilon^2 + (12\cos\tau + 4\cos 3\tau)\epsilon^3}{18\omega^2[9 + 12\epsilon\cos\tau + 2\epsilon^2(1 + \cos 2\tau)]} \tag{26}$$

Here $F(\tau)$ is periodic with period 2π. Thus Floquet theory tells us that the resulting Hill's equation on $z(\tau)$ will have solutions of period 2π or 4π on its transition curves. Now from Eq. (25), the boundedness of $z(\tau)$ is equivalent to the boundedness of $x(\tau)$, so transition curves for the z equation occur for the same parameters as do those for the x Eq. (20). Also, since the coefficient $\sqrt{3 + 2\epsilon\cos\tau}$ in Eq. (25) has period 2π, we may conclude that Eq. (20) has solutions of period 2π or 4π on its transition curves. Now when $\epsilon = 0$, Eq. (20) is of the form $x'' + \frac{1}{3\omega^2}x = 0$, and has solutions of period $2\pi\sqrt{3}\omega$. These will correspond to solutions of period 2π or 4π when $2\pi\sqrt{3}\omega = \frac{4\pi}{n}$, since a solution with period $\frac{4\pi}{n}$ may also be thought of as having period 2π (n even) or 4π (n odd), which gives $\omega = \frac{2}{n\sqrt{3}}$, $n = 1,2,3,\ldots$

To reiterate, we have shown that we can expect Eq. (20) to have tongues of instability emanating from the points $\omega = \frac{2}{n\sqrt{3}}$, $n = 1,2,3,\ldots$ on the ω-axis in the ω–ϵ parameter plane.

5. Perturbation method

In order to obtain approximate expressions for the transition curves of Eq. (20) in the ω–ϵ plane, we use a perturbation method valid for small values of ϵ [12,9]. We begin by looking for a transition curve through the point $\omega = \frac{2}{n\sqrt{3}}$, $\epsilon = 0$ in the form of a power series in ϵ:

$$\omega = \frac{2}{n\sqrt{3}} + k_1\epsilon + k_2\epsilon^2 + \cdots \tag{27}$$

where n is a positive integer. We also expand x in a series,

$$x(\tau) = x_0(\tau) + x_1(\tau)\epsilon + x_2(\tau)\epsilon^2 + \cdots \tag{28}$$

and substitute (27) and (28) into (20), collect terms and equate to zero the coefficient of each power of ϵ. For example, in the case of $n = 1$ we obtain for the first three equations:

$$x_0'' + \frac{1}{4}x_0 = 0 \tag{29}$$

$$x_1'' + \frac{1}{4}x_1 = -\frac{2}{3}x_0''\cos\tau - \frac{2}{3}x_0'\sin\tau + \frac{\sqrt{3}}{4}k_1x_0 - \frac{1}{3}x_0\cos\tau \tag{30}$$

$$x_2'' + \frac{1}{4}x_2 = -\frac{2}{3}x_1''\cos\tau - \frac{2}{3}x_1'\sin\tau + \frac{\sqrt{3}}{4}k_1x_1 - \frac{1}{3}x_1\cos\tau + \left(\frac{1}{\sqrt{3}}k_1\cos\tau + \frac{\sqrt{3}}{4}k_2 - \frac{9}{16}k_1^2 - \frac{1}{9}\cos^2\tau\right)x_0 \tag{31}$$

To solve these equations recursively we begin by taking the solution of Eq. (29) as

$$x_0 = \sin\frac{\tau}{2} \tag{32}$$

Substituting this into Eq. (30) and simplifying, we obtain:

$$x_1'' + \frac{1}{4}x_1 = \left(-\frac{1}{12} + \frac{\sqrt{3}}{4}k_1\right)\sin\frac{\tau}{2} - \frac{1}{4}\sin\frac{3\tau}{2} \tag{33}$$

For a solution $x(\tau)$ which is uniformly valid on the infinite interval we require no secular terms in x_1, i.e. we equate to zero the coefficient of $\sin\frac{\tau}{2}$ on the RHS of Eq. (33), giving:

$$k_1 = \frac{1}{3\sqrt{3}} \tag{34}$$

For this value of k_1, a particular solution to Eq. (33) is

$$x_1 = \frac{1}{8}\sin\frac{3\tau}{2} \tag{35}$$

Next Eqs. (34) and (35) are substituted into Eq. (31), and after trigonometric simplification, secular terms are removed, giving:

$$k_2 = -\frac{1}{72\sqrt{3}} \tag{36}$$

Substituting Eqs. (34) and (36) into (27), we have obtained the following expression for a transition curve:

$$n = 1 : \omega = \frac{2}{\sqrt{3}} + \frac{1}{3\sqrt{3}}\epsilon - \frac{1}{72\sqrt{3}}\epsilon^2 + O(\epsilon^3) \tag{37}$$

If instead of Eq. (32), we choose

$$x_0 = \cos\frac{\tau}{2} \tag{38}$$

and repeat the foregoing process, we obtain the following expression for another transition curve through the same point on the ϵ-axis:

$$n = 1 : \omega = \frac{2}{\sqrt{3}} - \frac{1}{3\sqrt{3}}\epsilon - \frac{1}{72\sqrt{3}}\epsilon^2 + O(\epsilon^3) \tag{39}$$

Taken together, Eqs. (37) and (39) represent a tongue of instability, see Fig. 6.

In a similar way,we may derive approximate equations for the boundaries of tongues of instability which emanate from each of the points $\omega = \frac{2}{n\sqrt{3}}$, $n = 1,2,3,\ldots$ on the ϵ-axis. Here are the results for the first few such tongues:

$$n = 1 : \omega = \frac{1}{\sqrt{3}}\left(2 + \frac{\epsilon}{3} - \frac{\epsilon^2}{72} - \frac{5\epsilon^3}{1728} + \frac{271\epsilon^4}{124416} - \frac{7885\epsilon^5}{8957952} + O(\epsilon^6)\right) \tag{40}$$

$$n = 1 : \omega = \frac{1}{\sqrt{3}}\left(2 - \frac{\epsilon}{3} - \frac{\epsilon^2}{72} + \frac{5\epsilon^3}{1728} + \frac{271\epsilon^4}{124416} + \frac{7885\epsilon^5}{8957952} + O(\epsilon^6)\right) \tag{41}$$

$$n = 2 : \omega = \frac{1}{\sqrt{3}}\left(1 - \frac{5\epsilon^2}{54} + \frac{13\epsilon^4}{34992} + O(\epsilon^6)\right) \tag{42}$$

$$n = 2 : \omega = \frac{1}{\sqrt{3}}\left(1 + \frac{\epsilon^2}{54} - \frac{35\epsilon^4}{34992} + O(\epsilon^6)\right) \tag{43}$$

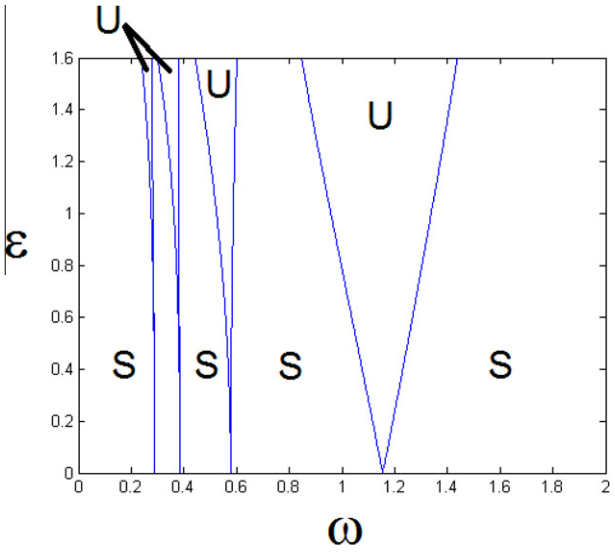

Fig. 6. Tongues of instability in the ω-ϵ plane. U = unstable, S = stable. Shown are those given by Eqs. (40)–(47). The region between the vertical ϵ axis and the first $n = 4$ transition curve (46) contains an infinite number of such tongues.

$$n=3:\omega=\frac{1}{\sqrt{3}}\left(\frac{2}{3}-\frac{\epsilon^2}{48}+\frac{\epsilon^3}{64}-\frac{217\epsilon^4}{61440}+\frac{11\epsilon^5}{16384}+O(\epsilon^6)\right) \tag{44}$$

$$n=3:\omega=\frac{1}{\sqrt{3}}\left(\frac{2}{3}-\frac{\epsilon^2}{48}-\frac{\epsilon^3}{64}-\frac{217\epsilon^4}{61440}-\frac{11\epsilon^5}{16384}+O(\epsilon^6)\right) \tag{45}$$

$$n=4:\omega=\frac{1}{\sqrt{3}}\left(\frac{1}{2}-\frac{2\epsilon^2}{135}-\frac{2032\epsilon^4}{273375}+O(\epsilon^6)\right) \tag{46}$$

$$n=4:\omega=\frac{1}{\sqrt{3}}\left(\frac{1}{2}-\frac{2\epsilon^2}{135}+\frac{968\epsilon^4}{273375}+O(\epsilon^6)\right) \tag{47}$$

6. Numerical simulation

In this section we check the foregoing perturbation results by using numerical integration. We begin by constructing a fundamental solution matrix for Eqs. (18) and (19) out of two solution vectors, $\begin{bmatrix}x_1(t)\\y_1(t)\end{bmatrix}$ and $\begin{bmatrix}x_2(t)\\y_2(t)\end{bmatrix}$, which satisfy the initial conditions:

$$\begin{bmatrix}x_1(0)\\y_1(0)\end{bmatrix}=\begin{bmatrix}1\\0\end{bmatrix},\quad \begin{bmatrix}x_2(0)\\y_2(0)\end{bmatrix}=\begin{bmatrix}0\\1\end{bmatrix} \tag{48}$$

From Floquet theory [9,12] we know that stability is determined by the eigenvalues of the fundamental solution matrix evaluated at time T:

$$C=\begin{bmatrix}x_1(T) & x_2(T)\\ y_1(T) & y_2(T)\end{bmatrix} \tag{49}$$

The eigenvalues of C satisfy the equation:

$$\lambda^2-(\mathrm{tr}C)\lambda+\det C=0 \tag{50}$$

where tr$C$ and det$C$ are the trace and determinant of C. Now Eqs. (18) and (19) have the special property that det$C$ = 1. This may be shown by defining W (the Wronskian) as:

$$W(t)=\det C=x_1(t)y_2(t)-x_2(t)y_1(t) \tag{51}$$

Taking the time derivative of W and using Eqs. (18) and (19) gives that $\frac{dW}{dt}=0$, which implies that $W(t)$ = constant = $W(0)$ = 1. Thus Eq. (50) can be written:

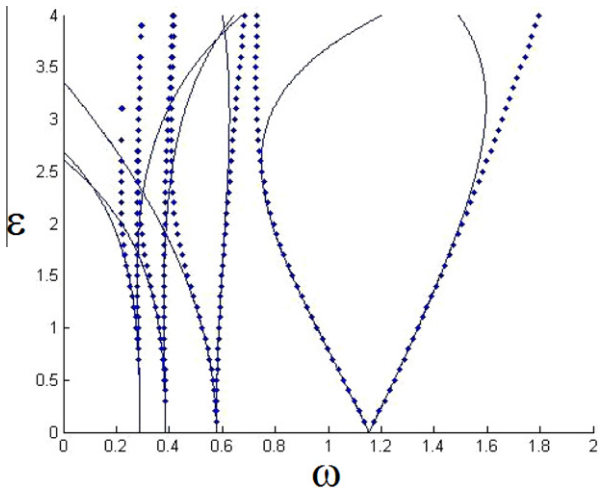

Fig. 7. Comparison of stability results obtained by numerical integration (dots) and by perturbation series (solid lines). The perturbation results are seen to lose accuracy for values of ϵ larger than about 1.5. Cf. Fig. 6.

$$\lambda^2 - (\mathrm{tr}C)\lambda + 1 = 0 \tag{52}$$

which has the solution:

$$\lambda = \frac{\mathrm{tr}C \pm \sqrt{\mathrm{tr}C^2 - 4}}{2} \tag{53}$$

Floquet theory tells us that instability results if either eigenvalue has modulus larger than unity [9,12]. Thus if $|\mathrm{tr}C| > 2$, then (53) gives real roots. But the product of the roots is unity, so if one root has modulus less than unity, the other has modulus greater than unity, with the result that this case is UNSTABLE and corresponds to exponential growth in time. On the other hand, if $|\mathrm{tr}C| < 2$, then (53) gives a pair of complex conjugate roots. But since their product must be unity, they must both lie on the unit circle, with the result that this case is STABLE.

Thus the transition from stable to unstable corresponds to those parameter values which give $|\mathrm{tr}C| = 2$. Note that this approach allows us to draw conclusions about the large time behavior after numerically integrating for only one forcing period.

The results of our numerical integrations are shown in Fig. 7. The perturbation results are verified for values of ϵ up to about 1.5.

7. Conclusions

In the traditional RPS scenario given by the payoff matrix (1), or by (6) with $\epsilon = 0$, it is possible to achieve a stable steady state in which all three populations are constant in time. If a small deviation from this equilibrium in initial conditions is presented, the resulting behavior of the system remains close to the equilibrium, with each population being nearly constant but with a small periodic variation in time. By contrast, if two of the payoff coefficients are permitted to depend periodically on time as in payoff matrix (6), there will exist certain combinations of parameters ω and ϵ for which a small deviation from equilibrium will cause the populations to differ considerably from the equilibrium state, and to vary quasiperiodically in time, see Fig. 5.

Quasiperiodic variation in population abundances is a common aspect of many biological systems. The model presented here shows how periodic variation in payoff coefficients (representing phenomena such as seasonal changes in fitness) can lead to such quasiperiodic population dynamics. For example, consider the side-blotched lizard *Uta stansburiana* [11]. The empirically observed lizard populations show quasiperiodic variation in abundance of the three types. Previously, these oscillations were explained by stochastic effects consistently perturbing the system away from stable coexistence. Our results suggest that instead, the observed lizard population dynamics could be explained by periodic variation in payoffs.

Acknowledgement

DGR gratefully acknowledges financial support from the John Templeton Foundation's Foundational Questions in Evolutionary Biology Prize Fellowship.

References

[1] Allahverdyan AE, Hu C-K. Replicators in a fine-grained environment: adaptation and polymorphism. Phys Rev Lett 2009;102:058102.
[2] Dreber A, Rand DG, Fudenberg D, Nowak MA. Winners don't punish. Nature 2008;452:348–51.
[3] Hofbauer J, Sigmund K. Evolutionary games and population dynamics. Cambridge UK: Cambridge Univ. Press; 1998.
[4] Kerr B, Riley MA, Feldman MW, Bohannan BJM. Local dispersal promotes biodiversity in a real-life game of rockpaperscissors. Nature 2002;418:171–4.
[5] Magnus W, Winkler S. Hill's equation. Dover; 1979.
[6] Nowak MA, Sigmund K. Evolutionary dynamics of biological games. Science 2004;303:793–9.
[7] Nowak MA. Evolutionary dynamics: exploring the equations of life. Cambridge MA: Harvard Univ. Press; 2006.
[8] Rand DG, Ohtsuki H, Nowak MA. Direct reciprocity with costly punishment: generous tit-for-tat prevails. J Theor Biol 2009;256:45–57.
[9] Rand RH. Lecture Notes in Nonlinear Vibrations, version 52, 2005, online at: <http://audiophile.tam.cornell.edu/randdocs/nlvibe52.pdf>.
[10] Schuster P, Sigmund K. Replicator dynamics. J Theor Biol 1983;100:533–8.
[11] Sinervo B, Lively CM. The rockpaperscissors game and the evolution of alternative male strategies. Nature 1996;380:240–3.
[12] Stoker J. Nonlinear vibrations in mechanical and electrical systems. Wiley; 1950.